



Analysis of Chromate-based Primers for Protection of Aluminium Alloys on Historical Aircraft

Magali Brunet, Luc Robbiola, Chantal Brouca-Cabarrecq & Philippe Sciau

To cite this article: Magali Brunet, Luc Robbiola, Chantal Brouca-Cabarrecq & Philippe Sciau (2022): Analysis of Chromate-based Primers for Protection of Aluminium Alloys on Historical Aircraft, *Studies in Conservation*, DOI: [10.1080/00393630.2022.2156037](https://doi.org/10.1080/00393630.2022.2156037)

To link to this article: <https://doi.org/10.1080/00393630.2022.2156037>



Published online: 21 Dec 2022.



Submit your article to this journal [↗](#)



View related articles [↗](#)



View Crossmark data [↗](#)

Analysis of Chromate-based Primers for Protection of Aluminium Alloys on Historical Aircraft

Magali Brunet¹, Luc Robbiola², Chantal Brouca-Cabarrecq¹ and Philippe Sciau¹

¹Centre d'Élaboration de Matériaux et d'Études Structurales, Centre National de la Recherche Scientifique, Université de Toulouse, Toulouse, France; ²Travaux et Recherches Archéologiques sur les Cultures, les Espaces et les Sociétés, Centre National de la Recherche Scientifique, Université de Toulouse, Toulouse, France

ABSTRACT

Immediately following the use of aluminium alloys, particularly Duralumin, in the construction of aircraft, protective coatings with anti-corrosion properties were developed. Among the numerous solutions to prevent corrosion, the most widely employed materials were organic primers containing chromates. This paper reports the study of the corrosion inhibitive compounds (chromates) used by aircraft manufacturers during World War II. More specifically, we have identified the nature of the compounds and assessed their current efficiency. Our analyses on samples collected from three different wrecks (French and German) excavated on terrestrial sites reveal that the primer contained either zinc tetroxychromate or lead chromate. Using XANES to study the chromium oxidation states elucidated the different phenomena taking place during the aging of the paint primer. We found that the reduction of Cr(VI) to Cr(III) species occurred either within the primer or at the interface of the primer with the Al alloy. This is believed to be due to alteration of the paint layer and its long exposure to the natural environment. However, even after 80 years, Cr(VI) is still present in the primers of these archaeological parts. Although a little altered, the chromate compound can still provide a source of inhibitor, thus maintaining the protection of the alloys.

ARTICLE HISTORY

Received May 2022
Accepted December 2022

KEYWORDS

Aluminium alloys; aircraft; cultural heritage; primer; chromates; XANES

Introduction

Duralumin, an alloy of aluminium with good mechanical properties (high strength and hardness), was developed by A. Wilm in 1906. The availability of this alloy gave great impetus to the general expansion of aeronautics shortly after World War I in strategic areas such as in the military industry and in civil transport (Carpentier 2012). However, very early in the history of the alloy, the low corrosion resistance of Duralumin was a major concern and developing solutions for its protection was a priority for engineers and scientists. The corrosion inhibitive properties of chromates were well-known in the area of metal protection (Kittelberger 1942) and consequently, one of the first solutions to protect Duralumin from corrosion was the addition of chromate pigments to a paint primer. Chromates could be associated with various cations, namely, zinc, potassium, potassium-zinc, barium, strontium, lead, etc. (Cole 1955). In parallel, different coating formulations involving chromates were also developed (Rousset-Bert 1958; Adams and Hallam 1991; Kendig and Buchheit 2003), such as chemical oxidation in alkaline baths (Modified Bauer and Vogel – MBV process) in the early 1920s, and soon after, chemical conversion coatings in acidic baths (also involving the use of phosphates) were reported.

Thus, the coatings present on the surface of aluminium on a historical aircraft could be very diverse and also quite complex (Merrick and Kiroff 2010). Unfortunately, manufacturers' archives are scarce, being either lost or destroyed. It is therefore difficult to identify the nature of the anti-corrosion treatments specifically used by a nation or by an aircraft manufacturer at a particular period in history.

In the abovementioned scenario, the precise identification of the chromate-based corrosion inhibiting compound is the first step in the study of primers that have been applied on aluminium alloys in historical aircraft. This information has to be then supplemented by a detailed study of the chromium oxidation states at areas very close to the surface of the aluminium substrate so as to determine how the anti-corrosion compound has changed with the passage of time. Such information could help in clarifying whether the corrosion protection provided by the chromate still remains still efficient. This question is indeed of major importance when considering the conservation of historical aircraft, which were left for decades buried or left on the ground and so more exposed to ambient air, which might have resulted in severe degradation of the coatings to create lifting, cracks, and blisters. Such degradation likely would have affected the

anti-corrosion layer too. Assessing the efficiency of the anticorrosion treatments will help in the preservation of this category of cultural heritage and in developing future restoration protocols.

Among the large corpus of World War II aircraft wrecks that we described in a previous work (Ouissi et al. 2019), there were only a few parts that still show remains of the original paint. Hence each painted specimen is a rare testimony of this period and it is therefore important to document and preserve these samples. In this article, with the aim to extend our knowledge of anticorrosion treatments used in the past, we collected three samples from excavated wrecks. Two were French aircraft (a fighter Dewoitine D.520 (1940) and a sea-plane Latécoère 298 (1940)), and the third was a German fighter aircraft, a Heinkel 111 (1937). With these samples, we focused our investigation on the primer, i.e. the first layer that is in contact with the metal and which enables the corrosion inhibitive effect. Using spectroscopic and microscopic laboratory analyses, i.e. scanning electron microscopy with energy-dispersive X-ray spectroscopy (SEM-EDX) coupled with Raman spectroscopy, it was possible to identify the corrosion inhibitive pigment in the primer. In addition, the oxidation state of chromium, which plays a major role in corrosion inhibition, was determined from synchrotron radiation-based techniques, i.e. micro X-ray fluorescence (μ -XRF) and microscale X-ray absorption near edge structure spectroscopy (μ -XANES). The latter technique has proven to be efficient for understanding chromatic alterations of yellow pigments in paintings, for example, in Van Gogh (Monico et al. 2015) or Seurat's (Zanella et al. 2011) masterpieces. In the study of anticorrosion protection of aluminium alloys, XANES has also been used to study the mechanism of action of chromate in corrosion inhibition in chemical conversion coatings (CCC) (Kendig, Davenport, and Isaacs 1993; Le Bozec et al. 2003). In fact, hexavalent chromium Cr(VI) has a distinct pre-edge peak at 5993.5 eV linked to its tetrahedral coordination which enhances the 1s to 3d electronic transition probability. Cr(VI) can be easily distinguished from Cr(III) oxide which shows two small pre-edge peaks: a characteristic peak at 5990.5 eV and another between 5993.1 and 5994.5 eV depending on the compound (Monico et al. 2016; Monico et al. 2020). Another advantage of the XANES technique is that it is performed in ambient air and hence change in valence state of the active species due to high vacuum can be avoided.

In the present work, we show that depending on the manufacturer, different chromate-based pigments have been used as corrosion inhibitors on historical samples. Moreover, as it will be reported in the discussion, the characterisation of the different chemical states of chromium on each sample provides

information on the alteration of the protective coatings and as to how far this protection is still effective.

Materials and methods

The samples studied in this work are composed of aluminium alloys covered with a protective coating to resist corrosion (primer) on which one or more coatings of paint are present. All the samples come from wrecks excavated in the Pyrenees (south of France) and buried in a terrestrial environment. They were only brushed after excavation. The samples with residues of paint were selected after visually observing the surface of the archaeological remains. For convenience, the samples of coated aluminium alloys studied in this work are named as follows: DE520 for Dewoitine D.520, LA298 for Latécoère 298, and HE111 for Heinkel 111.

The residues of paint shown in Figure 1 are representative and characteristic of each aircraft: beige (chamois) for Dewoitine, blue for Latécoère, and green for Heinkel. Table 1 lists the elemental composition of the bulk aluminium alloy in the three samples. DE520 and the HE111 are mainly Duralumin alloys (typically 3.5–5% of Cu, 0.5–1% of Mg, 0.5% of Mn, and 0.5% of Si) whereas that of LA298 shows some specific differences. Although the copper and magnesium contents are close to those of Duralumin, no manganese was detected and other elements such as zinc, chromium, and nickel are present in minor amounts.

Each coated sample was first observed by optical microscopy, after which it was cut, embedded in epoxy resin, and polished first on SiC papers and then on a cloth with diamond paste up to 1 μ m grade to obtain a mirror-like finish. On the polished cross-sections, the coating stratigraphy could be observed by optical microscopy.

Energy dispersive X-ray spectroscopy (EDX) performed on an Oxford X-Max^N 150 spectrometer, coupled to a scanning electron microscope (SEM) on a FEI Helios Nanolab 600i operating at 20 kV was used to identify the elements present in the layers of paint and to determine the elemental composition of the substrate, i.e. the aluminium alloy. We acquired EDX data on four 500 \times 500 μ m² areas with a minimum of 10⁶ counts on each spectrum. Before each measurement, the beam intensity was optimised with respect to a pure Co standard. Quantitative analysis was performed with internal standards (pure K-line Al, Si, and Fe standards) and results were normalised to 100 wt%. Raman spectroscopy, that combines optical microscopy with spectrometry, was performed using an XploRA[®] spectrometer from Horiba. A green laser at 532 nm was used as the excitation source. The combination of the two techniques (SEM-EDX and Raman) enabled identification of the nature of the pigments

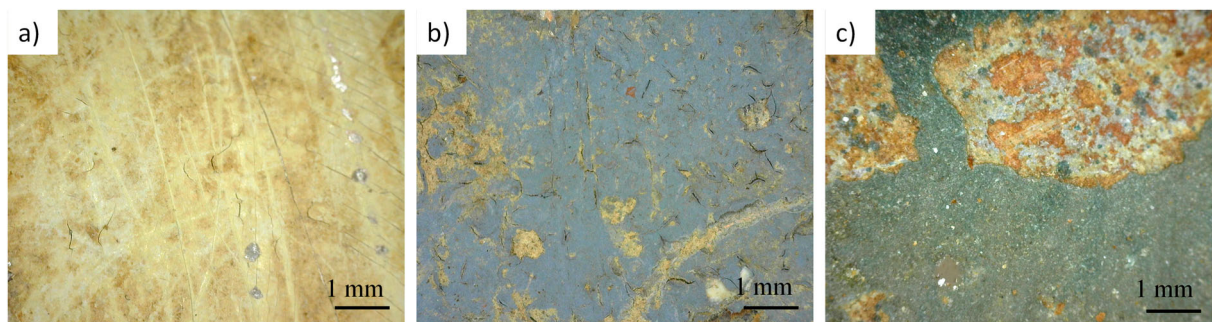


Figure 1. Optical microscopy images of the paints on each of the samples: (a) DE520, (b) LA298, (c) HE111.

and other inorganic compounds such as fillers present in the protective coatings.

Experiments were then conducted on the same embedded samples at SOLEIL synchrotron facilities on the beamline LUCIA (Line for Ultimate Characterisation by Imaging and Absorption) using 800–8000 eV monochromatic X-ray microprobe (micron size) adapted for X-ray absorption spectroscopy (μ -XAS) and elemental mapping by μ -XRF. On each sample, XRF maps (each with $\sim 100 \mu\text{m} \times 50 \mu\text{m}$ area) were acquired at 6100 eV energy to locate areas containing chromium. PyMcaTM software was used to plot the elemental maps. Next, XANES spectra for Cr element were acquired at the points of interest (POI) that showed higher contents of Cr or across the Cr-Al interface. The acquisition was in reflection mode in the energy range from 5950 eV to 6100 eV. Energy steps were adapted to obtain well defined pre-edge peaks: 2 eV in the range 5950 eV – 5986 eV (below the pre-edge peak), 0.2 eV in the range 5986 eV–6014 eV (around the pre-edge peak), 0.5 eV in the 6014 eV–6040, and 1 eV up to 6100 eV. After acquisition, the spectra were normalised using the DemeterTM suite (AthenaTM software).

Results

General observations and identification of corrosion inhibiting compounds

Initial macroscopic observation on the surface of all the samples (see Figure 1) highlights alterations in the paint layers which present cracks, blisters, and delamination. Such alterations are mainly linked to their aging (>80 years). On the outermost surface of the

sample HE111, concretions are also present, due to its buried state.

Figures 2 and 3 present the images and analyses acquired by optical microscopy and SEM-EDX on the cross-sections of the three samples. For all the samples, the primer is the red layer that is in direct contact with the aluminium alloy. The SEM-EDX study showed that for the two French aircraft (DE520 and LA298), Cr element is associated with Zn and K inside the red primer layer forming the pink species in the EDX maps of Figures 2a and b. On LA298, a thin layer of Cr only correlated to O was homogeneously distributed on the surface of the alloy over the entire sample. As for the paint layers, both DE520 and LA298 samples contain Ti-O (TiO₂) as a mineral filler. Cr was also found in the paint layer of LA298 associated with Pb and O.

The sample HE111 is composed of four layers as seen in Figure 1c: the red primer, a metallic grey layer (hereafter denoted as layer 1), a light green layer, and a darker green layer. Two representative zones were studied: zone H1 reported in Figure 3a, where only the red primer and the metallic grey layer (layer 1) are conserved and in Figure 3b, the zone H2, where the primer is not clearly observed with a concretion layer replacing the primer/paint. The EDX mapping on zone H1 (see Figure 3a), shows that the red primer contains micron-size platelets (parallel to the surface) with Si, Mg, and O elements. This compound was identified as talc based on X-ray diffraction data (not reported here), a common mineral filler used by German manufacturers. Three submicronic phases were also detected containing: Cr-O-Pb (corresponding to the inhibitive pigment), Fe-O, and Zn-O elements. Between the two zones, H1 (with primer and paint) and H2 (with only the concretion layer), we performed EDX mapping, shown in Figure 3b, to reveal the transition between the two zones. Our results revealed that the concretion layer is composed of three phases of different elemental composition including: K-Si-O, Si-O, and Fe-O or Ca-Al-O (probably from the soil). In the zone H2, Cr element was only rarely present and in very few areas underneath the concretion layer.

Table 1. Elemental composition in normalised weight (wt.%) measured by SEM-EDX analysis on polished cross-sections (estimated error 10% for minor elements).

Sample	Elemental composition (wt%)								
	Al	Cu	Mg	Mn	Fe	Si	Zn	Cr	Ni
DE520	93.2	4.4	0.5	0.6	0.3	0.5	–	–	–
LA298	93.3	3.8	0.7	0.0	0.4	0.4	0.5	0.6	0.4
HE111	93.2	4.3	0.6	0.8	0.3	0.5	–	–	–

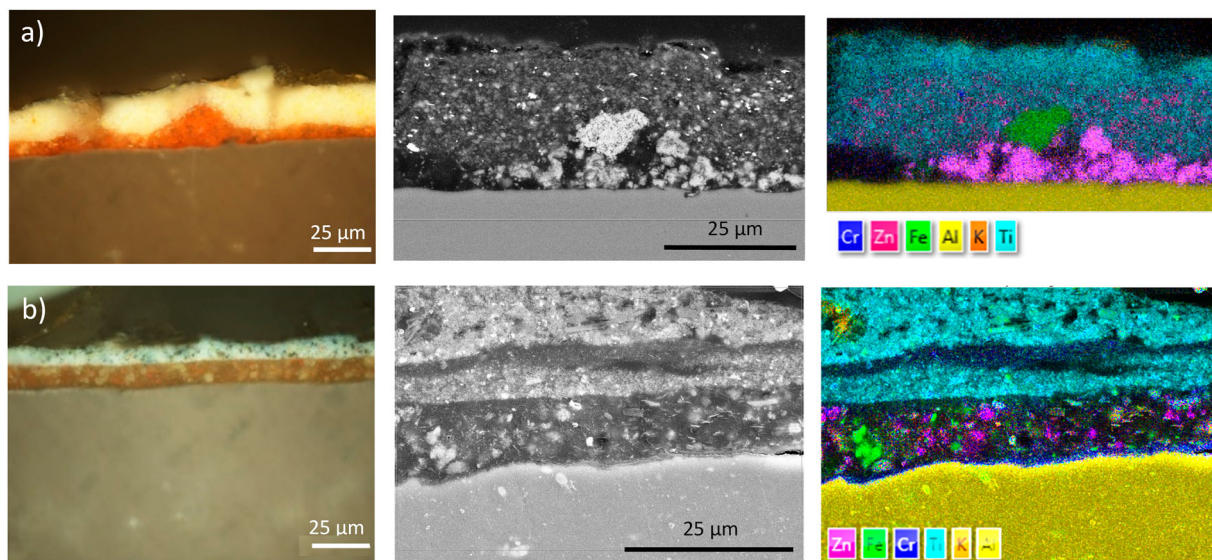


Figure 2. Protective coating of samples (a) DE520 and (b) LA298 in cross-section: optical microscopy images (left column), SEM-BEI images (middle column) and SEM-EDX mapping (right column) with Cr (dark blue), Zn (red magenta), Fe (green), Al (yellow), K (orange), and Ti (light blue).

We used Raman spectroscopy to identify chromate-containing crystals both in the primer and the paint layer. As shown in the spectra of [Figure 4a](#), the pigment $4\text{ZnCrO}_4 \cdot \text{K}_2\text{O} \cdot 3\text{H}_2\text{O}$ (zinc tetroxychromate) was identified in the primer present in the two French aircraft samples (DE520 and LA298): the strong peak at 872 cm^{-1} corresponds to the CrO₄ group (v₁) stretching. Other peaks at 343 w, 357 w (shoulder), 372 w, 407 w, 771 w, 892, and 941 cm^{-1} are also typical of this compound (Bell, Clark, and Gibbs 1997). Zinc tetroxychromate ($4\text{ZnCrO}_4 \cdot \text{K}_2\text{O} \cdot 3\text{H}_2\text{O}$) is a well-known pigment that was developed in the nineteenth century (Otero et al. 2017). This

compound was tested as a corrosion inhibitive pigment in the early 1940s (Kittelberger 1942) and proved to be an excellent inhibitor as well as being resistant to humidity. Hence, it has been widely used in the aeronautics industry as a corrosion inhibitor for aluminium alloys, particularly in France (Meynis de Paulin 1947; Rousset-Bert 1958). The red colour of the primer was attributed to the presence of Fe_2O_3 (hematite). On the sample LA298, due to the very small thickness of the Cr-O layer, no Raman spectrum could be collected at the interface.

In the sample HE111, as shown in the [Figure 4b](#), the identified Cr-compound in the primer was PbCrO_4

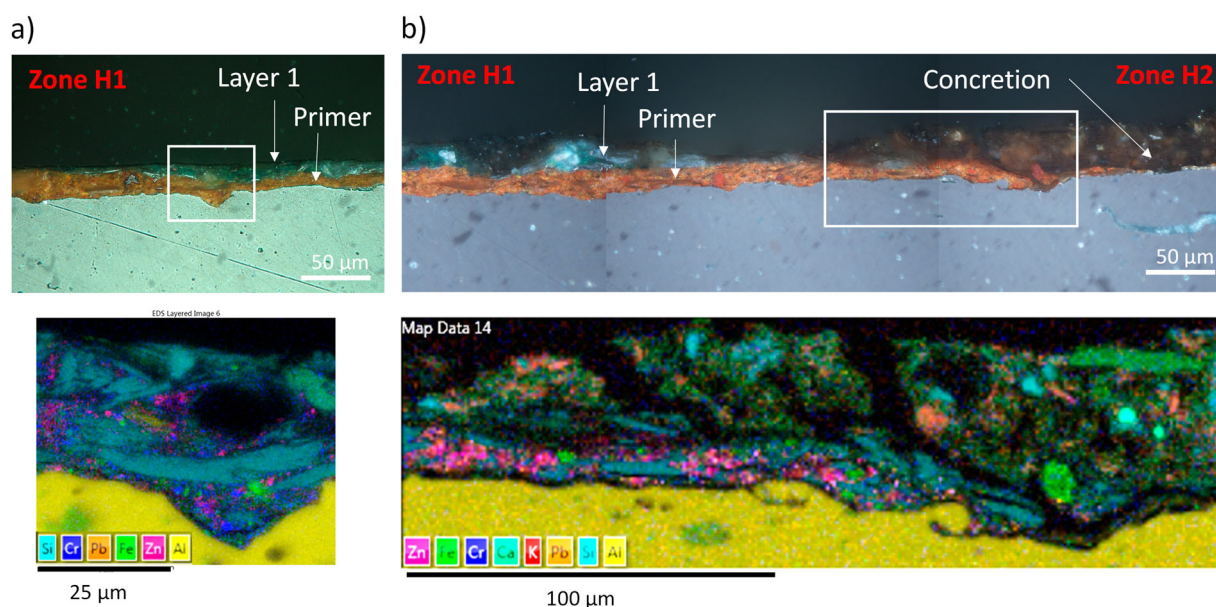


Figure 3. Protective coating of sample HE111 in cross-section observed by optical microscopy and analysed by SEM-EDX showing (a) zone H1. Inset: EDX maps with Cr (dark blue), Zn (red magenta), Fe (green), Al (yellow), Pb (orange), Si (light blue); and (b) intermediate zone between H1 and H2 zones. Inset: EDX maps with additional elements K (red), and Ca (turquoise).

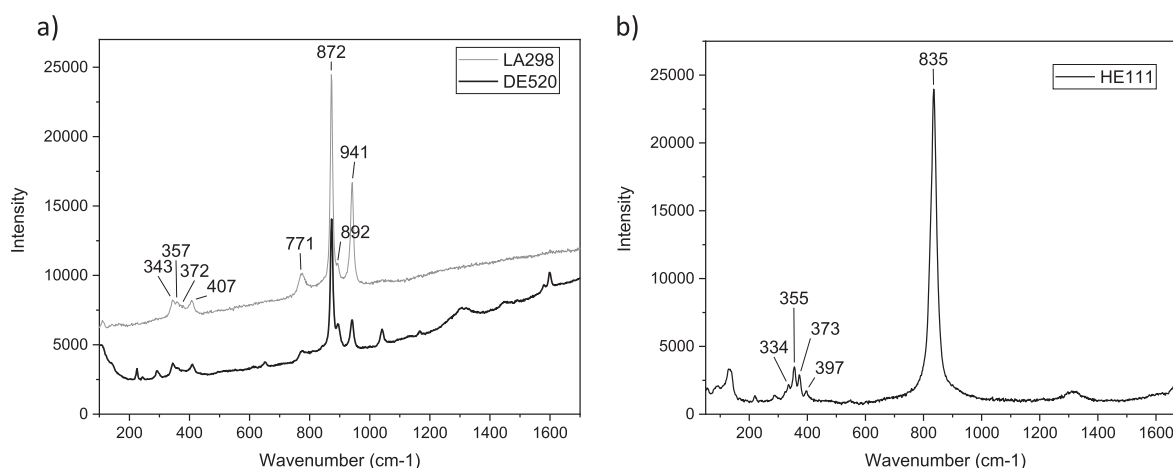


Figure 4. Raman spectrum on a crystal in the primer layer of (a) DE520 and LA298 samples and (b) HE111 sample.

(crocoite). A main peak is found around 835 cm⁻¹ corresponding to the stretching (ν_1) of the CrO₄ group in lead chromates, as for instance, crocoite. The other peaks at 334, 355, 373, and 397 cm⁻¹ confirm the identification of crocoite (Burgio and Clark 2001; Frost 2004). Compared to zinc chromates, the CrO₄ stretching mode in crocoite is shifted to a lower wavenumber of 837 cm⁻¹ due to the presence of PbO (Bell, Clark, and Gibbs 1997). It should be pointed out here that in the LA298 paint layer, lead chromate (PbCrO₄) was also identified as the yellow pigment.

XANES investigation on cross-sections

Figure 5 shows the XRF maps and XANES data for the DE520 sample. A tri-colour (Ti, Cr, Al) map was chosen in order to visualise the interfaces (substrate/primer/paint) and select the point of analyses. XANES was

acquired on a line profile crossing the primer, from the points of interest POI 09 to POI 14 with steps of 2 μm in the Z direction. As shown in Figure 5b, all the XANES spectra are similar with a sharp pre-edge peak at 5993 eV. The height of the normalised pre-edge peak ($H\mu(5993)$) can be directly correlated to the proportion of Cr(VI) in the total chromium content which, as proposed by Zanella et al. (2011), follows the equation: $H\mu(5993) = (0.95 \pm 0.01) * x$, where x represents the fraction [Cr(VI)/Cr total]. We have plotted the reference sample with 100% Cr(VI) corresponding to Zn yellow ($\text{K}_2\text{O} \cdot 4\text{ZnCrO}_4 \cdot 3\text{H}_2\text{O}$) used by Zanella et al. along with our spectra. For the reference sample, the height of the normalised pre-edge peak ($H\mu(5993)$) is very close to 1. For the spectra measured on DE520, the height of the pre-edge peak lies between 0.78 and 0.84 indicating the predominant presence of Cr(VI)-containing species with a small

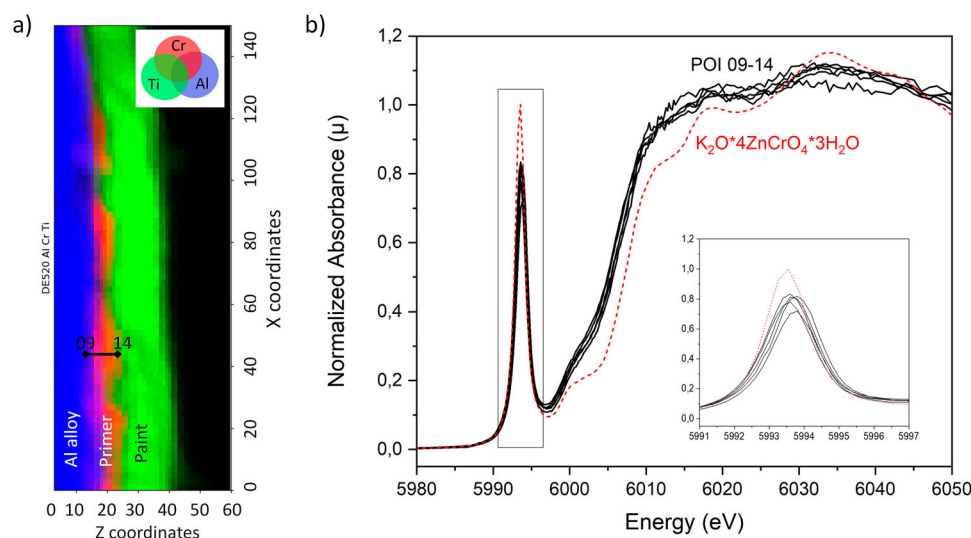


Figure 5. DE520 cross-section sample: (a) XRF (Cr, Ti, Al) map revealing the paint layer (green) and the primer (red) on the Al alloy (blue), with POI profile line (from 09 to 14); and (b) the corresponding normalised XANES spectra across the Al/primer interface. Inset: close-up view of the pre-edge peak at 5993.5 cm⁻¹. Spectrum of the reference zinc yellow pigment $\text{K}_2\text{O} \cdot 4\text{ZnCrO}_4 \cdot 3\text{H}_2\text{O}$ (courtesy of J.F. Gaillard) is also shown (dashed line).

amount of Cr(III) species. The rest of the spectra (from 5594 eV to 6020 eV) is in good agreement with that observed for the reference sample with 75% Cr(VI): 25% Cr(III) reported by the same authors (Zanella et al. 2011).

Similar XRF maps were acquired for the LA298 sample, (see Figure 6a). The XANES spectra measured across the primer: from POI 10 to POI 23 (with a step of 1 μm) together with the reference Zn yellow spectrum are plotted in Figure 6b. An additional spectrum for POI 06 showing a typical Cr(0) (chromium metal) behaviour was acquired. This clearly confirms the presence of Cr as a minor element (i.e. higher than 0.1 wt.%) in the alloy as determined from the SEM-EDX analysis (Table 1). Next, on the profile line of the primer from POI 10 to POI 23, a mixture of Cr(III) and Cr(VI) was found. Figure 7 plots the Cr(VI) intensity over the maximum intensity extracted from the reference Zn yellow spectrum ($H\mu(5993)$) versus the distance (in micrometres): POI 10 corresponds to 0 μm and POI 23–13 μm . This shows that at the interface with the metal, the Cr(III) content is significantly greater than Cr(VI), i.e. $\text{Cr(VI)}/\text{Cr total} \sim 0.25$; the Cr(VI) content increases reaching a maximum with a ratio of 0.67 in the primer layer at the interface with the paint. A lower height of the Cr(VI) peak is observed in the paint, with a normalised intensity around 0.5, related to the change of cation in the chromate compound (zinc chromate \Rightarrow lead chromate) earlier identified by Raman spectroscopy.

For the HE111 sample, different elements were chosen to construct tri-colour maps of the interfaces, as shown in Figures 8a and 9a. These include Al, Cr, and Si for the H1 zone, Si being representative of talc which is largely present in layer 1, and Al, Cr, and Ca for the H2 zone since Ca is one of the elements present in the concretion layer. For the H1 zone

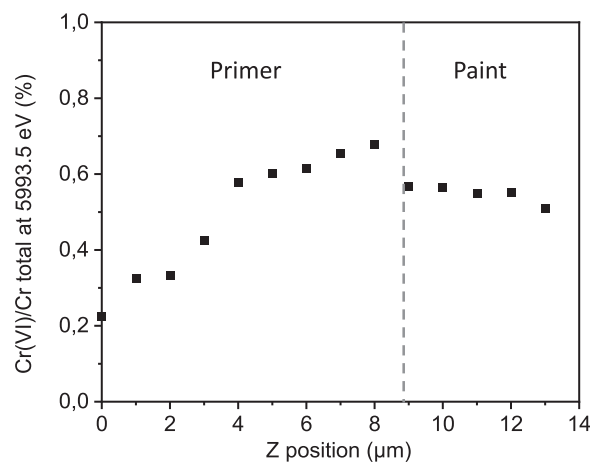


Figure 7. LA298 cross-section sample – Evolution of the Cr(VI) peak intensity at 5993.5 eV normalised to (Cr total) ($H\mu(5993)$) within the primer from POI 10 (0 μm) to POI 23 (13 μm).

where the primer is still present, as shown in Figure 8, the XANES spectra across the primer interface (from POI 09 to POI 13, step 2 μm) exhibit the same behaviour all the way from the alloy up to the concretion layer (see Figure 8b) showing a mixture of Cr(III) and Cr(VI) with Cr(VI) being preponderant; the height of the pre-edge peak ($H\mu(5993)$) on the normalised spectrum was between 0.6 and 0.7.

For the H2 zone, Figure 9b shows the XANES spectra in the primer, from POI 01–05 (with steps of 3 μm). The spectra have a totally different shape to those of the H1 zone. Two pre-edge peaks at 5990.6 and 5993.5 eV are seen, evidencing the presence of a mixture of Cr(III) and Cr(VI), but with Cr(III) being predominant. The height of the first pre-edge peak appears to vary but this trend is not correlated to the distance of the POI from the interface primer/alloy.

As compared to reported XANES spectra for Cr_2O_3 reported in the literature (Zanella et al. 2011; Monico

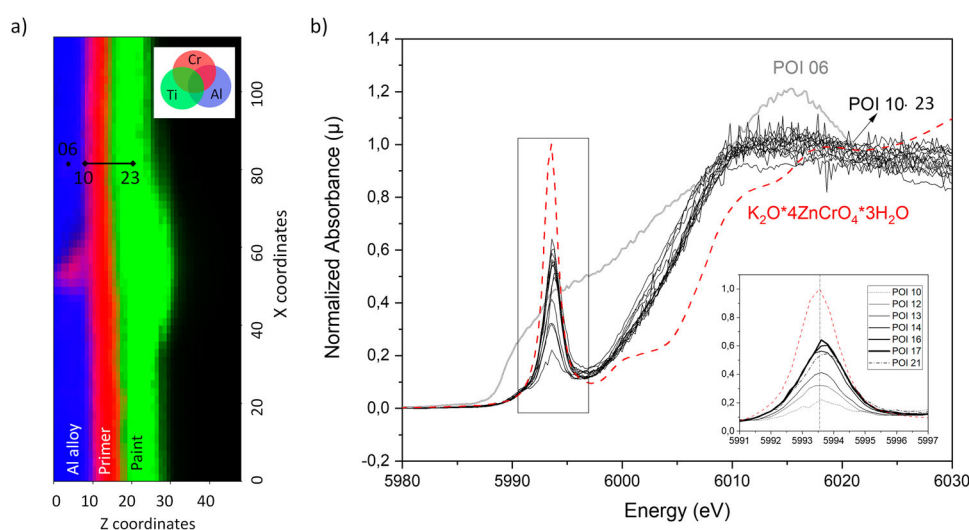


Figure 6. LA298 cross-section sample: (a) XRF (Cr, Ti, Al) map with POI 06 (in the Al alloy) and POIs from 10 to 23; (b) normalised XANES spectra across the Al/primer interface, POI 06 (Al alloy), POI 10–POI 11 (interface), and POI 14 (in the middle of the layer) plotted together with that of the reference Zn yellow (dashed line). Inset: close-up view of the pre-edge peak.

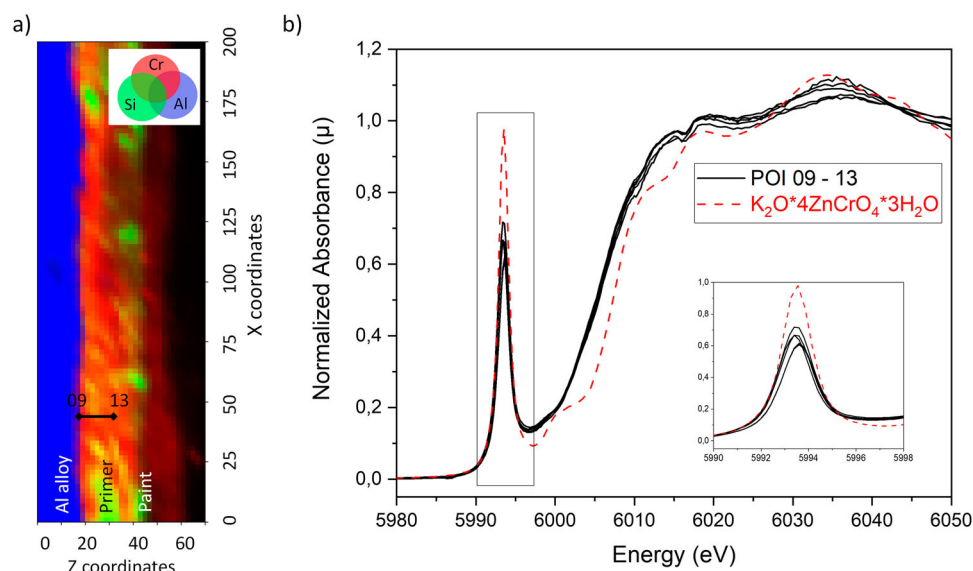


Figure 8. HE111-zone H1 cross section sample: (a) XRF (Cr, Si, Al) map with POIs from 09 to 13; (b) normalised XANES spectra across the Al/primer interface. The plot for the reference Zn yellow is shown by the dashed line. Inset: close-up view of the pre-edge peak.

et al. 2015; Monico et al. 2016), the spectra acquired in this H2 zone present significant differences. The usually reported second pre-edge peak at 5994.5 eV is not present (see insert of Figure 9b) and the post-edge shapes do not match. On the other hand, the XANES shape is similar to that previously reported for $\text{Cr}(\text{OH})_3$ (Papassiopi et al. 2014; Monico et al. 2020) indicating that the Cr(III) compound detected in the present case is not an oxide of chromium oxide but rather a hydroxide.

Discussion

The analysis of the three primers applied on WWII aircraft by spectroscopic and microscopic techniques

(SEM-EDX coupled with Raman) allowed identification of two corrosion inhibitive pigments, namely, zinc tetroxychromate ($\text{K}_2\text{O}\cdot 4\text{ZnCrO}_4\cdot 3\text{H}_2\text{O}$) for the two French aircraft (DE520 and LA298) and lead chromate (PbCrO_4) for the German aircraft (HE111). From XANES measurements across the interfaces of the investigated samples, we identified three different oxidation states of chromium, namely, Cr(0), Cr(VI), and Cr(III).

We noted several cases where Cr(III) species was present locally. First, in the DE520 sample, a small proportion of Cr(III) with mainly Cr(VI) was found across the primer thickness (Figure 5), which we believe is linked to the degradation of chromate within the primer, as already shown in another reported work (Monico et al. 2015). In the LA298 sample, a similar process was

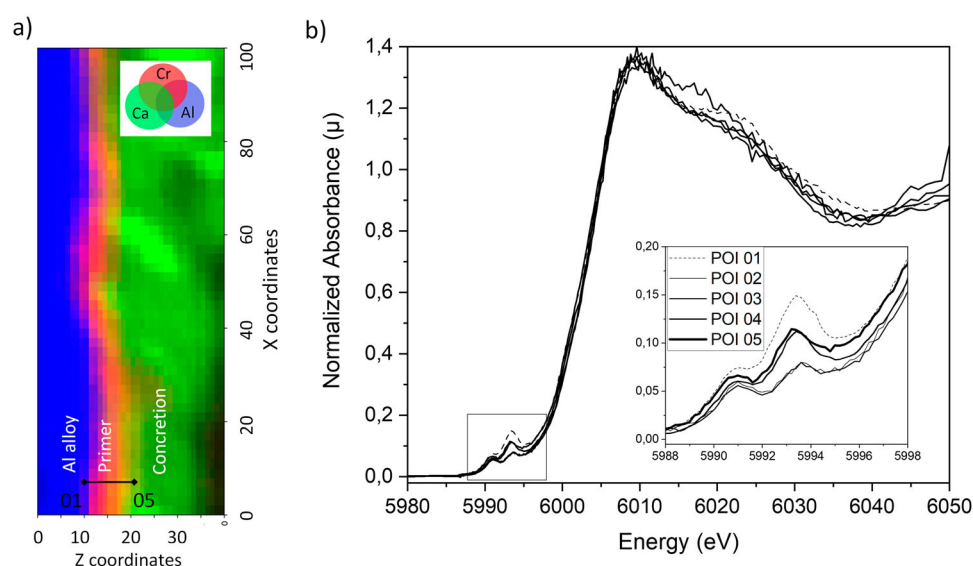


Figure 9. HE111-zone H2 cross-section sample: (a) XRF (Cr, Ca, Al) map with POIs from 01 to 05 and (b) normalised XANES spectra across the Al/concretion interface. Inset: close-up view of the pre-edge peak.

observed in the paint layer. The pre-edge peak intensity of around 0.5 for Cr(VI) in the paint layer could be due to an alteration of the chromate compound.

At the primer/Al alloy interface of the LA298 sample, as evidenced in Figure 6, Cr(III) is clearly present forming a thin internal sub-layer of the primer. No signal was found in Raman spectra taken in this zone to substantiate this conclusion, but the sensitivity of the Raman signal for Cr(III) is known to be lower than for Cr(VI) (Zhao, Frankel, and McCreery 1998). It is possible that different types of Cr(III) compounds were present. From the XANES spectra (Figure 6), we infer that chromium oxide (Cr_2O_3) is not prevalent but instead, a complex form such as chromium hydroxide is more likely to be present. Considering that this Cr(III)-containing sub-layer is homogeneous on the sample and within a primer that has remained intact but mainly containing Cr(VI), several hypotheses can be made. The presence of the Cr(III)-containing sub-layer could be due either to a specific treatment applied prior the deposition of the primer such as a flash primer, or to a process similar to chromate conversion coatings (CCC). The second possibility is that the primer/paint layers were degraded due to ageing during the long period of time the wreck was on the ground and exposed to the elements. In this ageing process, the penetration of humidity could have occurred first uniformly across the paint layer and then the primer, inducing leaching of Cr(VI) oxyanions from the primer. Subsequently, the following reactions are possible, as already reported in (Kendig, Davenport, and Isaacs 1993; Zhao, Frankel, and McCreery 1998; Frankel 2001): migration of the chromate species (CrO_4^{2-} , HCrO_4^- , or $\text{Cr}_2\text{O}_7^{2-}$ depending on the pH) and its adsorption on the active corrosion sites of aluminium (pits). In contact with the $\text{Al}(\text{OH})_x$ at the surface and through the release of H^+ , the chromium species could then be reduced to the trivalent form, eventually resulting in a Cr(VI)/(Cr(III) mixed oxide at the metal surface.

For the HE111 sample, as observed by OM (Figure 3), the painting system (primer, paint) is altered, with the creation of *lacunae* and concretions. In the H1 zone, where the primer and one paint layer are still present, the XANES spectra (see Figure 8b) show that chromate is still in the form of Cr(VI), with a small proportion of Cr(III) and only a minor alteration in composition is seen. In the H2 zone where Ca-containing concretions covered the alloy surface, Cr element was only rarely spotted by SEM-EDX (see map of Figure 3b) but was detected by μ -XRF, as shown in Figure 9a. This proves that the primer was originally present and it underwent a chemical reaction. XANES spectra indicate the predominance of Cr(III). Thus, it is possible that, similar to the LA298 sample, even after the disappearance of the physical protective coating provided by the paint layer and the primer,

Cr(VI) originally present in the lead chromate pigment still effectively played its role as a corrosion inhibitor. Cr(VI) locally reacted with the aluminium substrate in the presence of ambient humidity producing chromium hydroxide Cr(III) at the alloy interface. This type of reaction has been experimentally demonstrated in the case of CCC on Al 2024 T3 alloy (Le Bozec et al. 2003) and for a chromate-containing protective paint system on the Al 2024-T3 alloy (Furman et al. 2006), which are in good concordance with the result obtained on coated Duralumin samples that have naturally aged since WWII.

Conclusions

A study of the chromate compounds found in the primers applied on Al alloys present in three different WWII aircraft was done combining SEM-EDX analysis, Raman spectroscopy, μ -XRF, and XANES. From the results on sample cross-sections, several conclusions can be made:

- In the two French aircraft, the Dewoitine D.520 (1940) and the sea-plane Latécoère 298 (1940), the corrosion inhibitive pigment in the primer was the well-known zinc tetroxychromate ($4\text{ZnCrO}_4 \cdot \text{K}_2\text{O} \cdot 3\text{H}_2\text{O}$), also used as a yellow pigment in contemporary paints. On the German aircraft, Heinkel 111 (1937), the pigment used for its anticorrosion properties was lead chromate (CrPbO_4).
- For all the three aircraft, inside the primer layer and when the primer was still covered with a paint layer, chromium was still hexavalent Cr(VI) but with a small proportion of trivalent chromium Cr(III). It is known that the slightly soluble hexavalent chromium provides a continuous timed release of inhibitor (Kendig and Buchheit 2003). Thus, we can deduce that after exposure to outdoor environment or burial for 80 years, although the chromate pigment is slightly altered, the corrosion inhibition properties of the primer are most probably maintained.
- On the other hand, wherever the coating is no longer a primer/paint layer, e.g. in the case of areas deficient in paint or *lacunae* as shown on the Heinkel aircraft, large amounts of Cr(III) species were found. This indicates that mostly all the Cr(VI) was reduced to Cr(III) species, forming a Cr(III) film (probably chromium hydroxide) which inhibited oxygen reduction (cathodic partial reaction). This Cr(III) film having a permanent corrosion inhibiting activity (Frankel 2001), it can be argued that passivation was ensured and the original aluminium substrate was still protected from corrosion.

However, to confirm these results, the corrosion inhibition efficiency of these old primers should be tested in laboratory experiments, i.e. in controlled corrosive environments simulating atmospheric conditions.

Acknowledgements

The samples were provided by the association Aérocherche for which we extend our special thanks to Gilles Collaveri. We also acknowledge SOLEIL for providing synchrotron radiation facilities and Delphine Vantelon for assistance in using the beamline LUCIA (Proposal 20200361). We would also like to thank Jean-François Gaillard who kindly provided the reference XANES spectrum of zinc yellow.

Disclosure statement

No potential conflict of interest was reported by the author(s).

ORCID

Magali Brunet  <http://orcid.org/0000-0002-2568-8046>

References

- Adams, C., and D. Hallam. 1991. "Finishes on Aluminium - A Conservation Perspective." In *Symposium '91: Saving the Twentieth Century, Ottawa, Canada*, edited by D. Grattan, 273–286. Ottawa: Canadian Conservation Institute.
- Bell, I. M., R. J. H. Clark, and P. J. Gibbs. 1997. "Raman Spectroscopic Library of Natural and Synthetic Pigments (pre- ≈ 1850 AD)." *Spectrochimica Acta Part A: Molecular and Biomolecular Spectroscopy* 53 (12): 2159–2179. doi:10.1016/S1386-1425(97)00140-6
- Burgio, L., and R. J. H. Clark. 2001. "Library of FT-Raman Spectra of Pigments, Minerals, Pigment Media and Varnishes, and Supplement to Existing Library of Raman Spectra of Pigments with Visible Excitation." *Spectrochimica Acta Part A: Molecular and Biomolecular Spectroscopy* 57 (7): 1491–1521. doi:10.1016/S1386-1425(00)00495-9
- Carpentier, J. 2012. "Cent vingt ans d'innovations en aéronautique." *Arts, Lettres et Sciences* 676: 1–733.
- Cole, H. G. 1955. "Tests on the Relative Efficiency of Chromate Pigments in Anticorrosive Primers." *Journal of Applied Chemistry* 5: 197–208. doi:10.1002/jctb.5010050501
- Frankel, G. S. 2001. *Mechanism of Al Alloy Corrosion and the Role of Chromate Inhibitors*. Columbus: Ohio State University Columbus Fontana Corrosion Center.
- Frost, R. L. 2004. "Raman Microscopy of Selected Chromate Minerals." *Journal of Raman Spectroscopy* 35 (2): 153–158. doi:10.1002/jrs.1121
- Furman, S. A., F. H. Scholes, A. E. Hughes, D. N. Jamieson, C. M. Macrae, and A. M. Glenn. 2006. "Corrosion in Artificial Defects. II. Chromate Reactions." *Corrosion Science* 48 (7): 1827–1847. doi:10.1016/j.corsci.2005.05.029
- Kendig, M. W., and R. G. Buchheit. 2003. "Corrosion Inhibition of Aluminum and Aluminum Alloys by Soluble Chromates, Chromate Coatings, and Chromate-Free Coatings." *Corrosion* 59 (5): 379–400. doi:10.5006/1.3277570
- Kendig, M. W., A. J. Davenport, and H. S. Isaacs. 1993. "The Mechanism of Corrosion Inhibition by Chromate Conversion Coatings from X-ray Absorption Near Edge Spectroscopy (Xanes)." *Corrosion Science* 34 (1): 41–49. doi:10.1016/0010-938X(93)90257-H
- Kittelberger, W. W. 1942. "Zinc Tetroxy Chromate, a Rust-Inhibitive Primer Pigment." *Industrial and Engineering Chemistry* 34 (3): 363–372. doi:10.1021/ie50387a026
- Le Bozec, N., S. Joiret, D. Thierry, and D. Persson. 2003. "The Role of Chromate Conversion Coating in the Filiform Corrosion of Coated Aluminum Alloys." *Journal of The Electrochemical Society* 150 (12): B561. doi:10.1149/1.1621413.
- Merrill, K. A., and J. Kiroff. 2010. *Luftwaffe Camouflage and Markings 1933-1945*. London: Ian Allan Publishing.
- Meynis de Paulin, J.-J. 1947. "La peinture de l'aluminium - Part 2." *Revue de l'Aluminium* 138: 325–331.
- Monico, L., M. Cotte, F. Vanmeert, L. Amidani, K. Janssens, G. Nuyts, J. Garrevoet, et al. 2020. "Damages Induced by Synchrotron Radiation-Based X-ray Microanalysis in Chrome Yellow Paints and Related Cr-Compounds: Assessment, Quantification, and Mitigation Strategies." *Analytical Chemistry* 92 (20): 14164–14173. doi:10.1021/acs.analchem.0c03251.
- Monico, L., K. Janssens, M. Alfeld, M. Cotte, F. Vanmeert, C. G. Ryan, G. Falkenberg, D. L. Howard, B. G. Brunetti, and C. Miliani. 2015. "Full spectral XANES imaging using the maia detector array as a new tool for the study of the Alteration Process of Chrome Yellow Pigments in Paintings by Vincent van Gogh." *Journal of Analytical Atomic Spectrometry* 30 (3): 613–626. doi:10.1039/C4JA00419A.
- Monico, L., K. Janssens, M. Cotte, L. Sorace, F. Vanmeert, B. G. Brunetti, and C. Miliani. 2016. "Chromium Speciation Methods and Infrared Spectroscopy for Studying the Chemical Reactivity of Lead Chromate-Based Pigments in oil Medium." *Microchemical Journal* 124: 272–282. doi:10.1016/j.microc.2015.08.028.
- Otero, V., M. F. Campos, J. V. Pinto, M. Vilarigues, L. Carlyle, and M. J. Melo. 2017. "Barium, Zinc and Strontium Yellows in Late 19th–Early 20th Century oil Paintings." *Heritage Science* 5 (1): 46. doi:10.1186/s40494-017-0160-3.
- Ouissi, T., G. Collaveri, P. Sciau, J.-M. Olivier, and M. Brunet. 2019. "Comparison of Aluminum Alloys from Aircraft of Four Nations Involved in the WWII Conflict Using Multiscale Analyses and Archival Study." *Heritage* 2 (4): 2784–2801. doi:10.3390/heritage2040172.
- Papassiopi, N., F. Pinakidou, M. Katsikini, G. S. E. Antipas, C. Christou, A. Xenidis, and E. C. Paloura. 2014. "A XAFS Study of Plain and Composite Iron(III) and Chromium(III) Hydroxides." *Chemosphere* 111: 169–176. doi:10.1016/j.chemosphere.2014.03.059.
- Rousset-Bert, P. 1958. "La Protection des Structures en Métal Léger Dans la Construction Aéronautique." *Corrosion et Anticorrosion* 6 (9): 74–89.
- Zanella, L., F. Casadio, K. A. Gray, R. Warta, Q. Ma, and J.-F. Gaillard. 2011. "The Darkening of Zinc Yellow: XANES Speciation of Chromium in Artist's Paints After Light and Chemical Exposures." *Journal of Analytical Atomic Spectrometry* 26 (5): 1090–1097. doi:10.1039/c0ja00151a.
- Zhao, J., G. Frankel, and R. L. McCreery. 1998. "Corrosion Protection of Untreated AA-2024-T3 in Chloride Solution by a Chromate Conversion Coating Monitored with Raman Spectroscopy." *Journal of The Electrochemical Society* 145 (7): 2258–2264. doi:10.1149/1.1838630